Comparison Between RSS Measurements and LBLRTM/CHARTS Calculations for Clear and Cloudy Conditions

E. J. Mlawer, J. S. Delamere, C. J. Scott, and S. A. Clough
Atmospheric and Environmental Research, Inc.
Cambridge, Massachusetts

L. C. Harrison, J. J. Michalsky, and P. W. Kiedron
Atmospheric Sciences Research Center
State University of New York at Albany
Albany, New York

H. W. Barker
Environment Canada

T. R. Shippert
Pacific Northwest National Laboratory
Richland, Washington

Introduction

Spectral measurements of solar radiation, such as those provided by the 512-channel Rotating Shadowband Spectroradiometer (RSS) (Harrison et al. 1999), have provided great illumination in the recent debate concerning the possibility of atmospheric absorption of solar radiation in clear skies in excess of that predicted by radiative transfer models. In particular, comparisons (Mlawer et al. 2000) between measurements taken by the RSS and calculations by Line-by-Line Radiative Transfer Model (LBLRTM) and Code for High resolution Accelerated Radiative Transfer and Scattering (CHARTS) (Moncet and Clough 1997) for 3 cases showed good agreement between the observations and calculations.

In this work, the method used in Mlawer et al. (2000) has been extended to the higher-resolution 1024-channel RSS for two clear-sky cases. Furthermore, RSS-1024 measurements taken in the presence of a stable, homogeneous, liquid cloud are compared with corresponding calculations by LBLRTM/CHARTS.

Clear-Sky Cases

The procedure used to compare clear-sky RSS measurements to LBLRTM/CHARTS calculations is detailed in Mlawer et al. (2000). Features of this procedure include:

- the measurements are scaled to provide consistency between RSS top of the atmosphere (TOA) solar irradiance values (from Langley analyses) and the solar source function used in the calculation, implying that the measurement-model comparisons are effectively between measured and calculated transmittances (expressed in irradiance units)

- the atmospheric profiles are obtained from sondes, with the H_2O column amount scaled to agree with that measured by the microwave radiometer (MWR) and the O_3 column amount scaled to agree with Total Ozone Mapping Experiment Spectrometer (TOMS)

- the aerosol optical depths in the calculation are calculated using an Angstrom relation derived from the ratio of (direct-beam) RSS measurements and LBLRTM calculations for transparent spectral elements

- a spectrally-constant aerosol single-scattering albedo is chosen to give optimal agreement between diffuse measurement and calculation

- the aerosol asymmetry parameter set to 0.7

For this work, the surface albedos used in the calculations were obtained by a different method than in Mlawer et al. (2000). First, measurements for the time period in question from the downlooking Multi-Filter Radiometers (MFRs) mounted on the 10m and 25m towers at the Southern Great Plains (SGP) Cloud and Radiation Testbed (CART) site are averaged. For each spectral channel on the instrument, these averages are then ratioed to the corresponding uplooking Multifilter Rotating Shadowband Radiometer (MFRSR) measurements of total irradiance to obtain a surface albedo. These surface albedo values, one for each of the six MFRSR channels, are then extended to the full RSS spectral domain (10000-28500 cm^{-1}) based upon observed spectral surface reflectances (Bowker et al. 1985). Due to possible inhomogeneities in surface type in the vicinity of the CART site, the spectral surface albedos obtained by this method may not be perfectly representative of the actual surface albedos that impact the observed downwelling diffuse irradiances and, therefore, are a potential contributor to measurement-model discrepancies.

The results of the comparison between RSS measurements and CHARTS calculations for March 20, 2000, at 17:26 Universal Time (UT) are shown in Figures 1 (direct irradiance) and 2 (diffuse irradiance). Similar comparisons for a low-sun case (23:30 UT) on the same day are shown in Figures 3 (direct) and 4 (diffuse). The direct irradiance differences for the two cases are small, with no evidence of any significant unknown absorption with spectral structure, i.e., absorption by molecules. The diffuse irradiance differences for the 17:26 case are highest in the spectral range 1000 to 14000 cm^{-1}, possibly a result of the derived Angstrom relation not fully accounting for the spectral behavior of the aerosol extinction. (The direct irradiance residuals in this spectral region show consistent behavior.) In addition, the value of aerosol single-scattering albedo needed for good agreement with the diffuse observations for this low-loading case is smaller than those usually assumed, consistent with the low loading case analyzed in Mlawer et al. (2000). It remains likely that the 'missing' absorption found in other studies for cases with low aerosol loading was due, in fact, to the aerosols. The diffuse residuals for the 23:30 UT case are more problematic, possibly a result of imperfect characterization of the sharply varying instrument cosine response function at large angles.
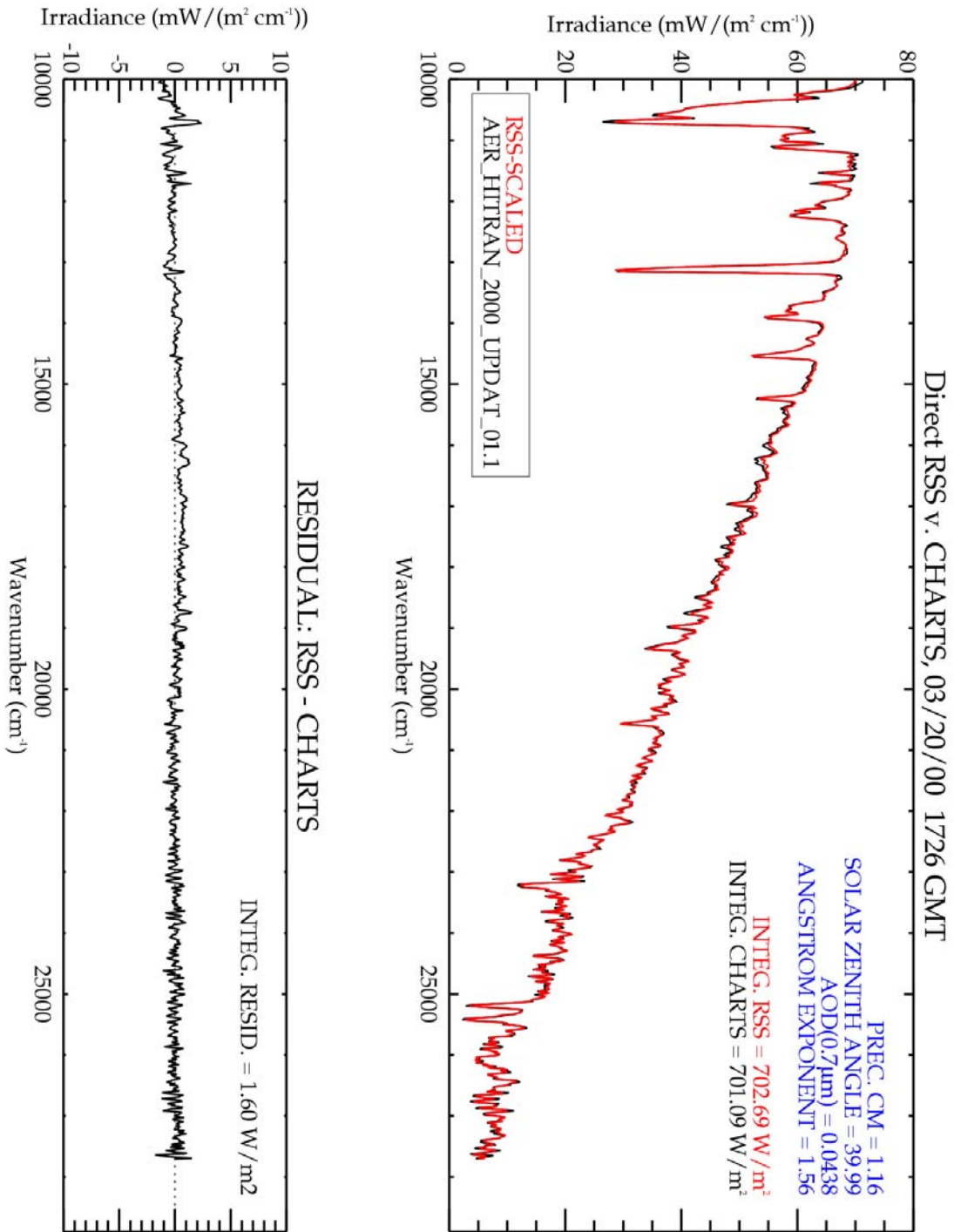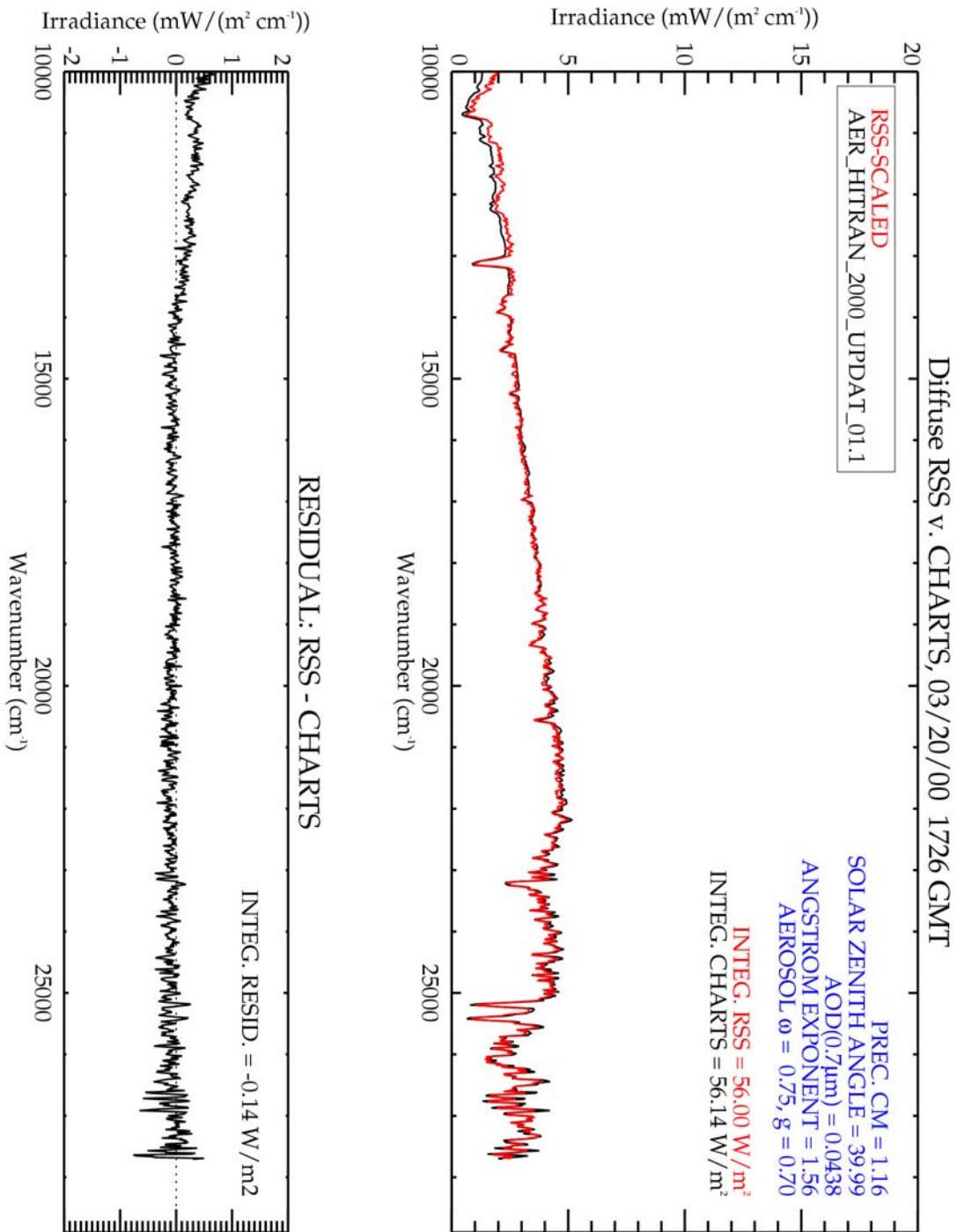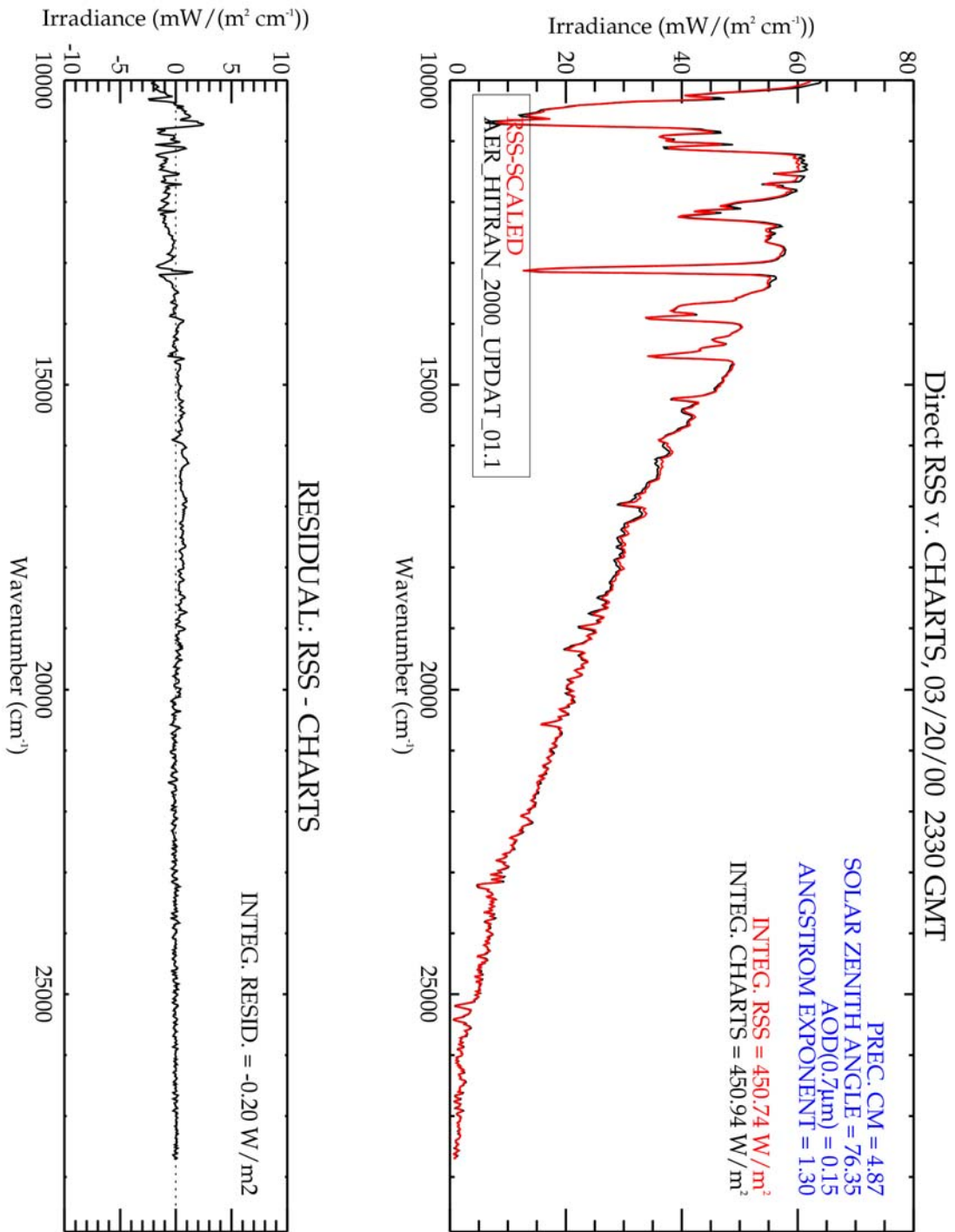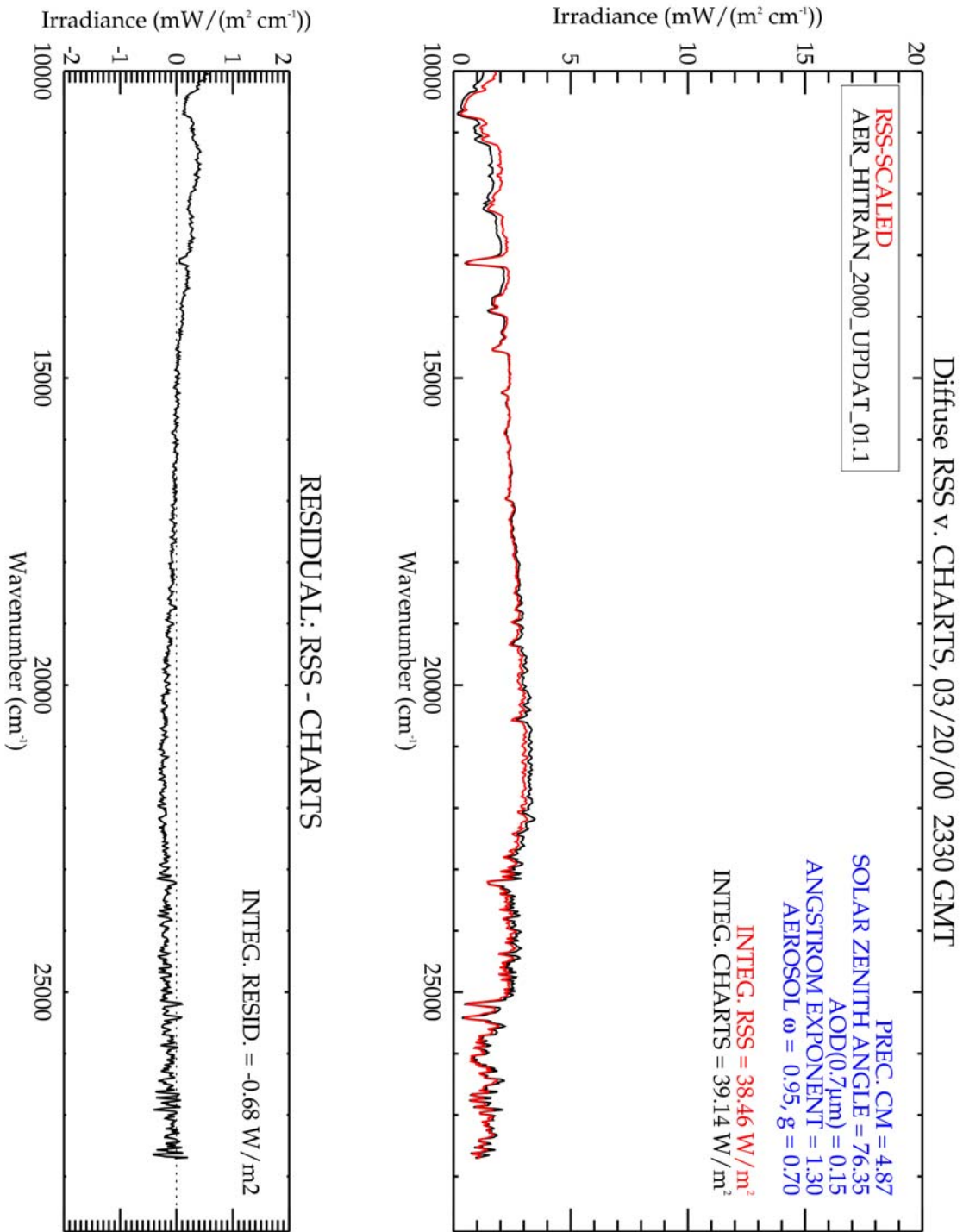
Figure 1.

Figure 2.

Figure 3.

Figure 4.

Adding Liquid Clouds

The Hu and Stamnes (1993) liquid cloud parameterization has been implemented in CHARTS. The results for two of the cloud cases from the recent intercomparison of radiative codes in climate models-III effort (Barker et al. 2002) have been compared to those from other multiple-scattering models and show good agreement (Figure 5) for the following cases: Cloud A - overcast low cloud, tropical atmosphere, cloud between 3.5 - 4 km, mixing ratio = 0.159 g/kg, visible optical depth of ~10; and Cloud B - overcast high cloud, tropical atmosphere, cloud between 10.5 - 11 km, mixing ratio = 0.034 g/kg, visible optical depth of ~1.

Cloudy Case Study

As shown in Figure 6, at ~16:00 UT on May 19, 2000, a low-level, horizontally-homogeneous, stable, stratocumulus cloud developed at the SGP CART site and persisted until ~20:00 UT. The diffuse irradiance measurements obtained at 17:00 UT by the 1024-channel RSS have been compared to corresponding calculations by CHARTS.

The input to the model was obtained as follows: (1) Cloud bottom (1.0 km) and top (1.5 km) were obtained from the Millimeter Cloud Radar (Figure 7); (2) Temperature and water vapor profiles are from the radiosonde released closest in time to 17:00 UT (Figure 8), with the water vapor column amount and cloud liquid water column amount (liquid water absorption was assumed to be constant within the cloud) being scaled to agree with the column amounts derived from MWR measurements (Figure 9); (3) Ozone column amount was obtained from TOMS; (4) Spectral surface albedos were obtained as described above (Figure 10); and (5) Aerosol optical depths were obtained from an Angstrom relation derived from the average of MFRSR aerosol optical depths measured during clear times on May 18 and May 20.

Figure 11 shows the comparison of diffuse observations and calculations using different values of effective radius of liquid water. The agreement for an effective radius of 9.0 μm is very good, both in terms of the integrated irradiance and, more importantly, the spectral behavior. The errors near 13000 cm^{-1} reflect the difficulties inherent in modeling the abruptly changing surface albedos in this spectral region.

Even though the lack of a measurement of upwelling radiation above the cloud makes difficult a definitive analysis concerning cloud absorption for this case, it is possible to use the RSS measurements and CHARTS calculations to investigate the sensitivity of the behavior shown in Figure 11 to the introduction in the model of a moderate amount of cloud absorption. For instance, a change in the single-scattering albedo of the liquid clouds from ~1.0 to 0.999 adds ~25 W/m^2 of cloud absorption in the RSS spectral region. Given the 'gray' nature of this change, it is not surprising that good spectral agreement can still be attained with an adjustment in the effective particle radius used in the calculation, specifically from 9.0 μm to 10.25 μm (Figure 12). Therefore, this RSS-CHARTS comparison cannot help assess the validity of extra cloud absorption if this absorption has no spectral content. However, recent results from the ARESE II campaign (Ellingson et al. 2001) are supportive of the existence of additional cloud absorption only in the near-infrared spectral region. To evaluate this possibility, the
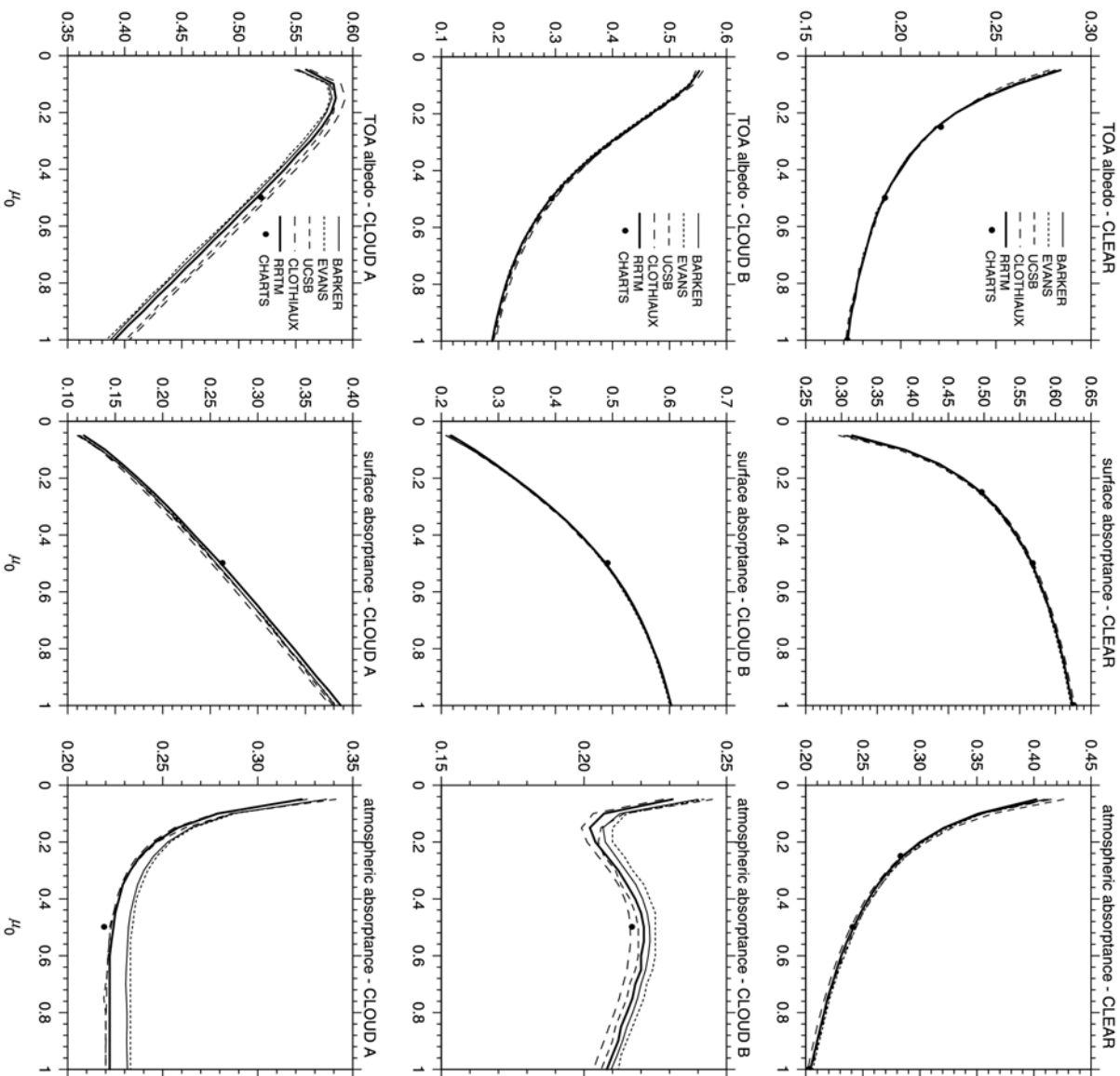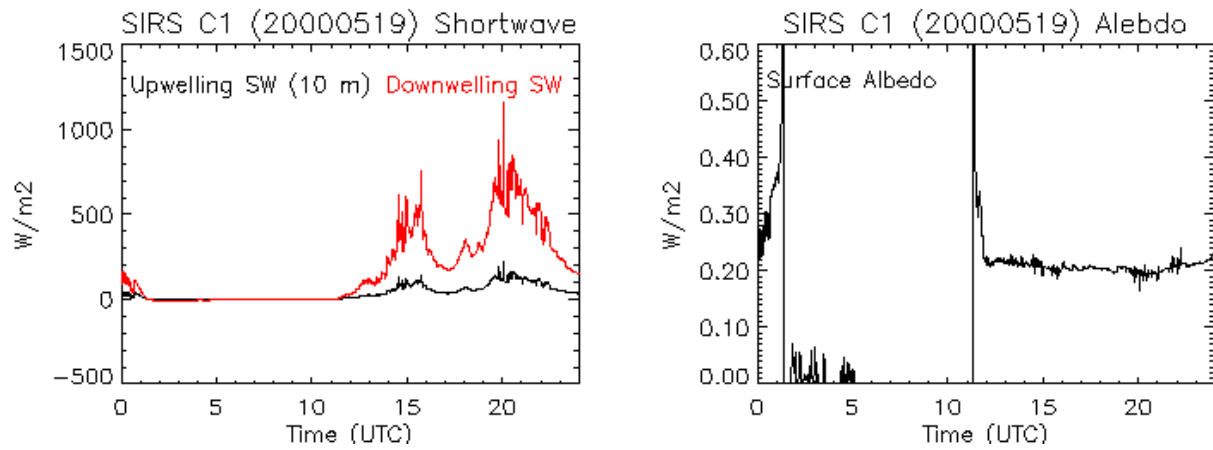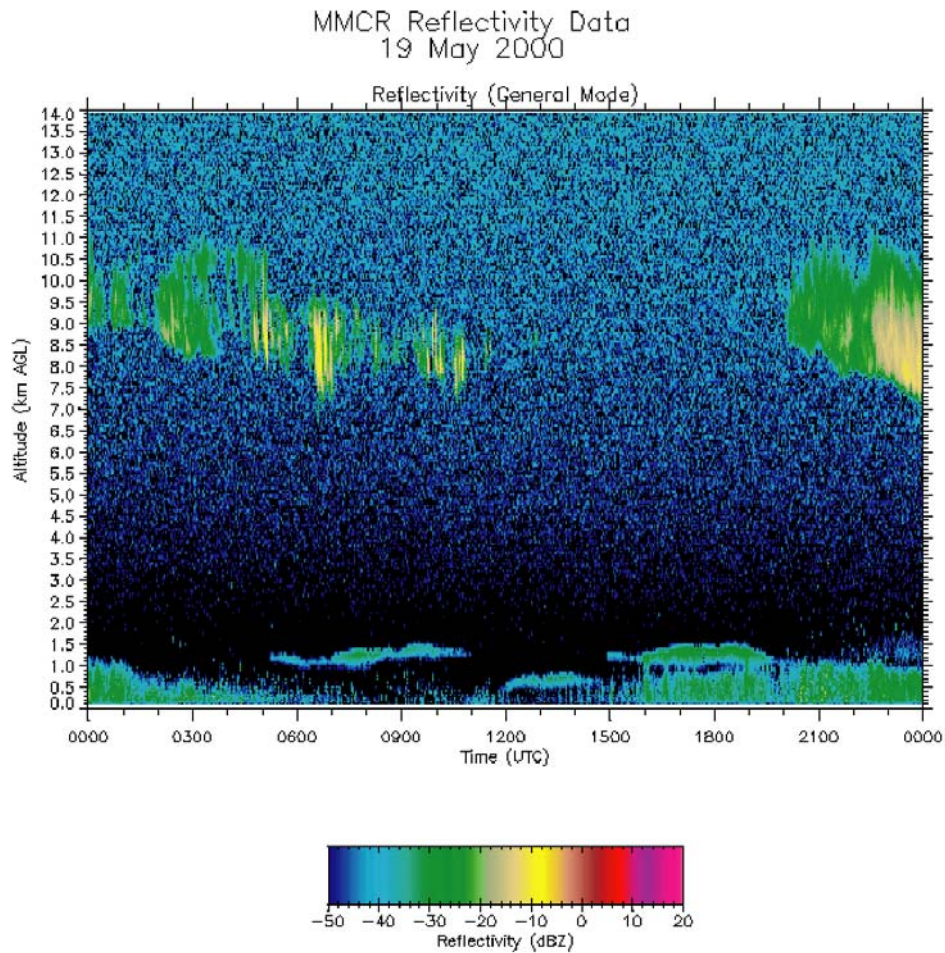
Figure 5.

Figure 6.

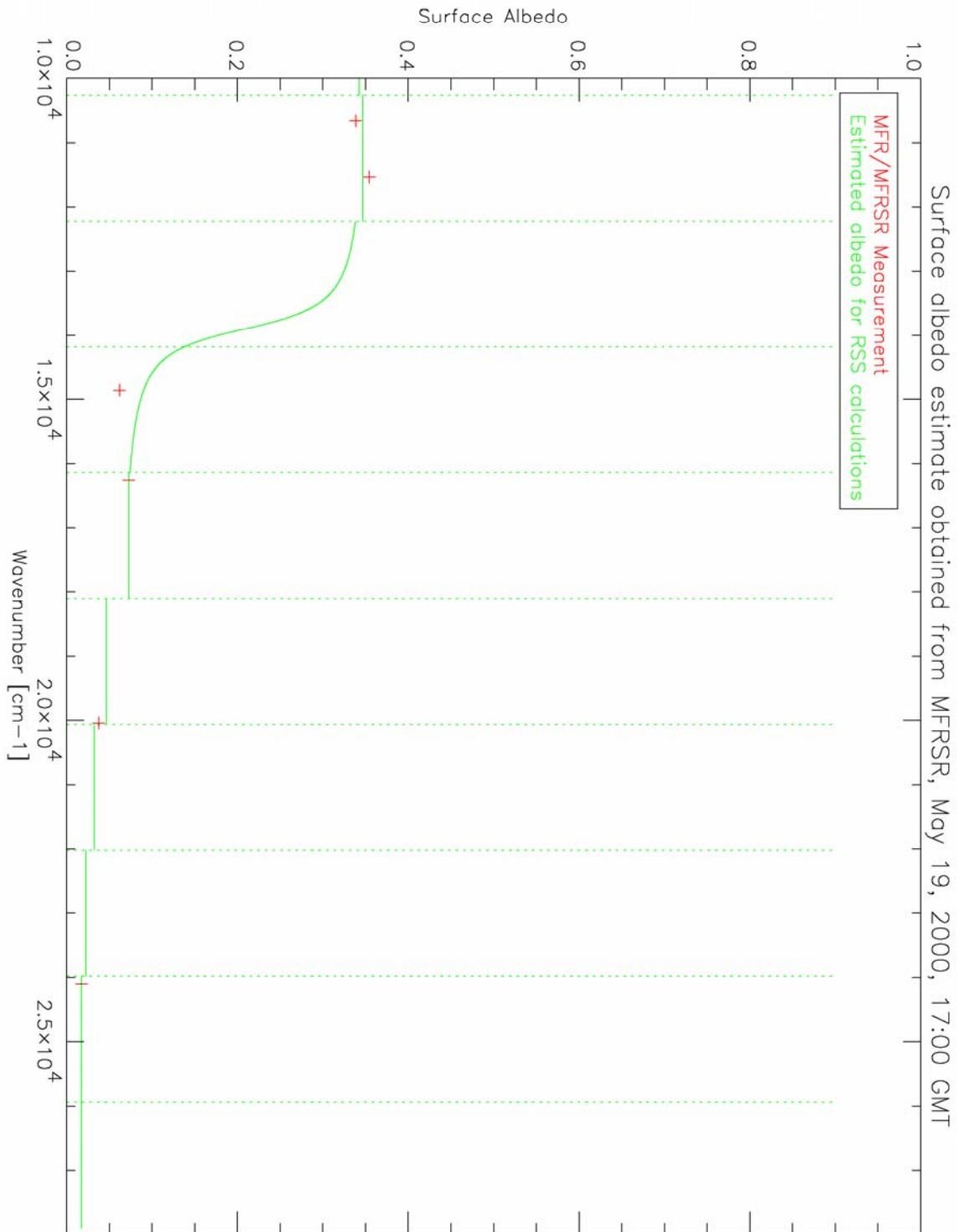**Figure 7**.
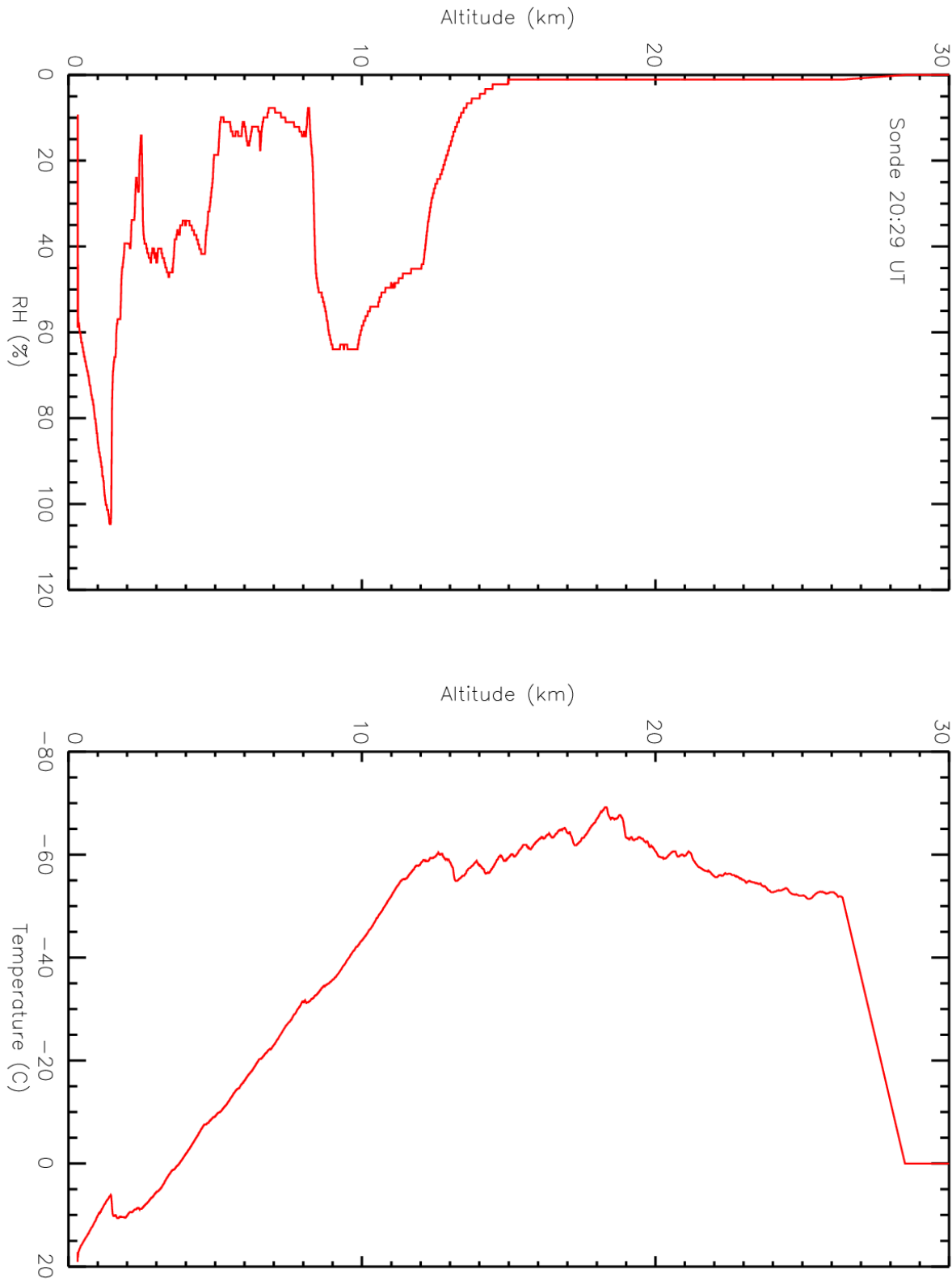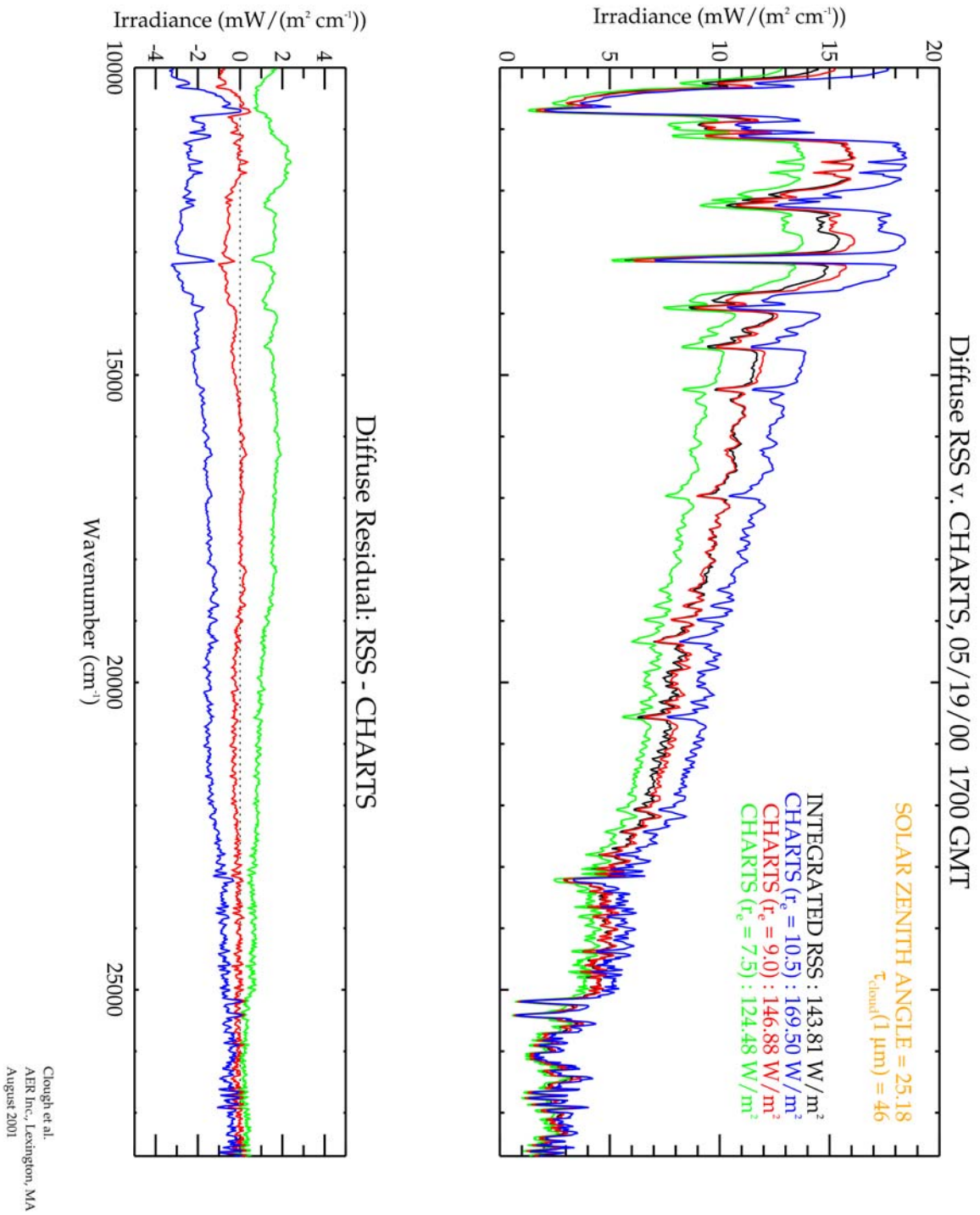
Figure 8.
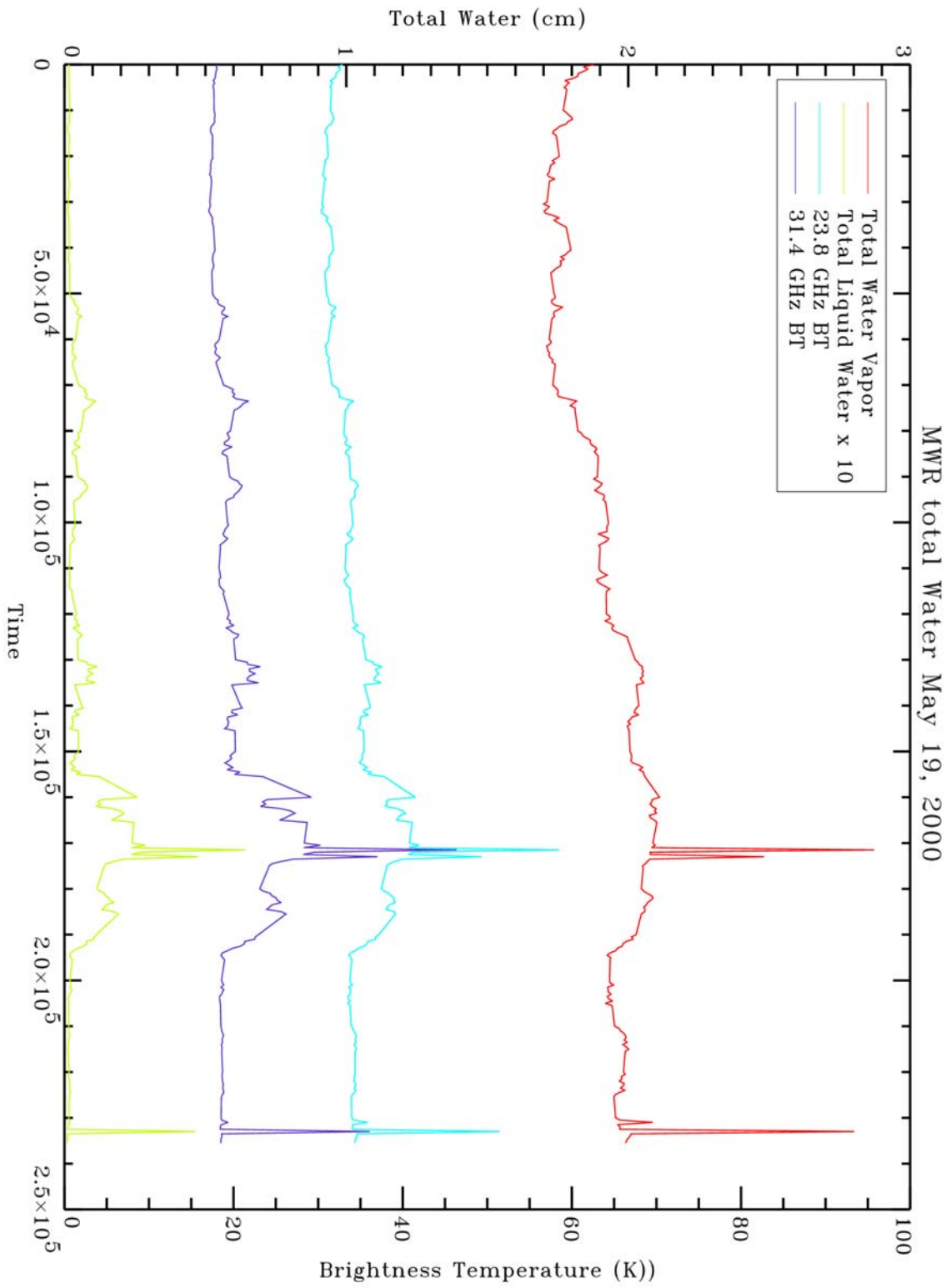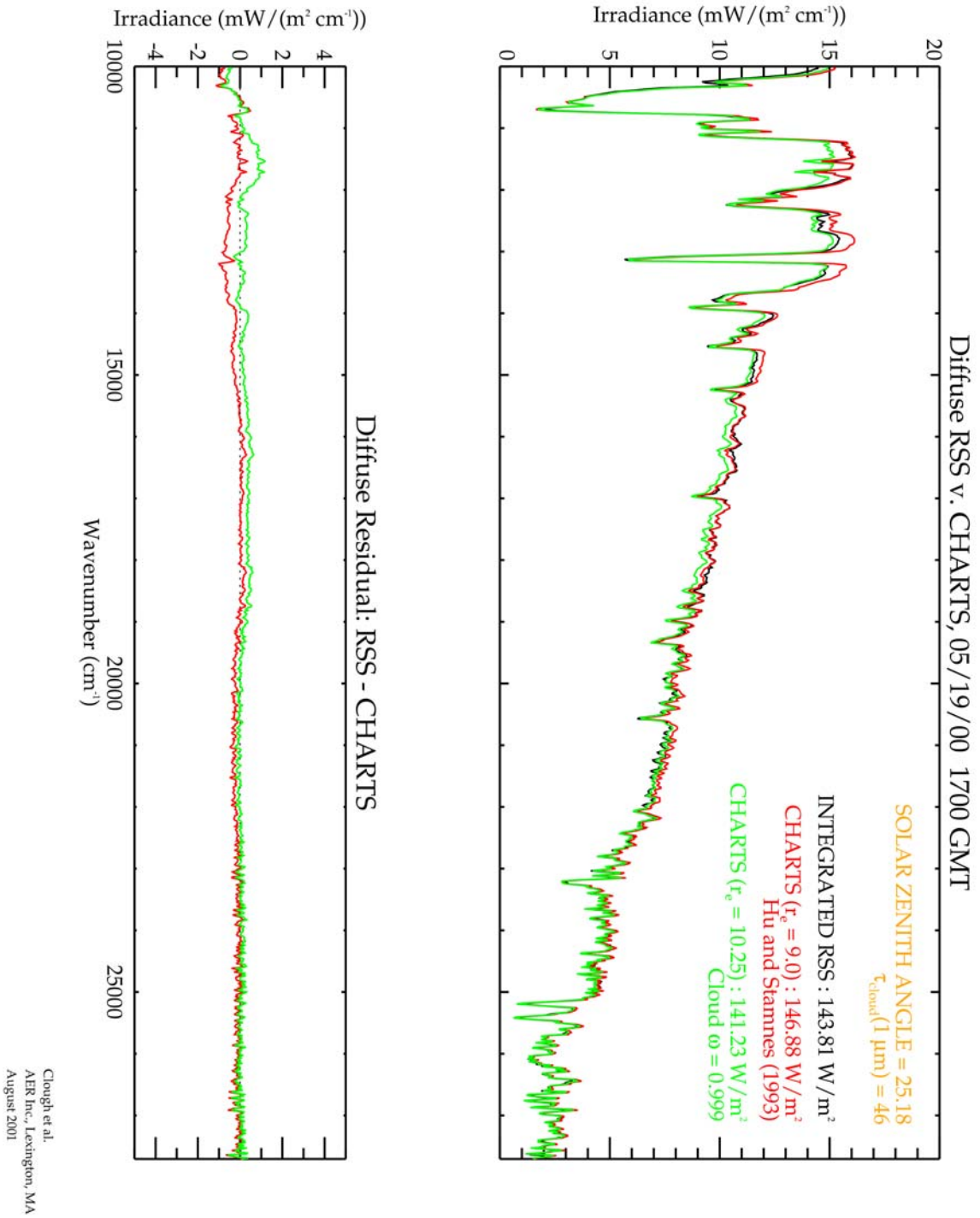
Figure 9.

Figure 10.

Figure 11.

Figure 12.

cloud single-scattering albedo was changed to 0.999 in the infrared and left unchanged in the visible (Figure 13), a change that adds an additional 25 W/m^2 of solar absorption by the cloud. Figure 14 shows the comparison between the RSS measurements and the CHARTS calculations using the cloud single-scattering albedos shown in Figure 13 and aneffective radiusof 9.0 µm (as in Figure 11). Clearly, this spectrally dependent change in single-scattering albedo leads to a large degradation in measurement-model agreement. Any attempt to improve the agreement in the near infrared by modifying the effective particle size would negatively impact the good agreement in the visible. This result provides compelling evidence that any additional cloud absorption present in the near infrared cannot be close to the magnitude depicted in Figure 13.

In conclusion, calculations of cloudy-sky spectral diffuse irradiances by CHARTS using the Hu and Stamnes (1993) liquid cloud parameterization and an effective radius of 9.0 µm are in good agreement with corresponding measurements obtained by the 1024-channel RSS. This good agreement can be maintained if spectrally gray cloud absorption is added, but not if a modest amount of cloud absorption is added only in the near-infrared spectral region.

Corresponding Author

Eli J. Mlawer, emlawer@aer.com, (781) 761-2226

Acknowledgments

References

Barker, H. W. et al. Assessing 1D atmospheric solar radiative transfer models: Interpretation and handling of unresolved clouds. *J. Geophys. Res.,* submitted.

Bowker, D. E., R. E. Davis, D. L. Myrick, K. Stacy, and W. T. Jones, 1985: Spectral reluctances of natural targets for use in remote sensing studies. *NASA Reference Publication* 1139.

Ellingson, R. G. et al., 2001: ARESE II: Description and Initial Results (ARM Enhanced Shortwave Experiment). This proceeding.

Harrison, L., M. Beauharnois, J. Berndt, P. Kiedron, J. Michalsky, and Q. Min, 1999: The Rotating Shadowband Spectroradiometer (RSS) and SGP. *Geophys. Res. Lett.,* **26**, 1715-1718.

Hu,.Y. X., and K. Stamnes, 1993: An accurate parameterization of the radiative properties of water clouds suitable for use in climate models. *J. Clim.*, **6**, 728-742.
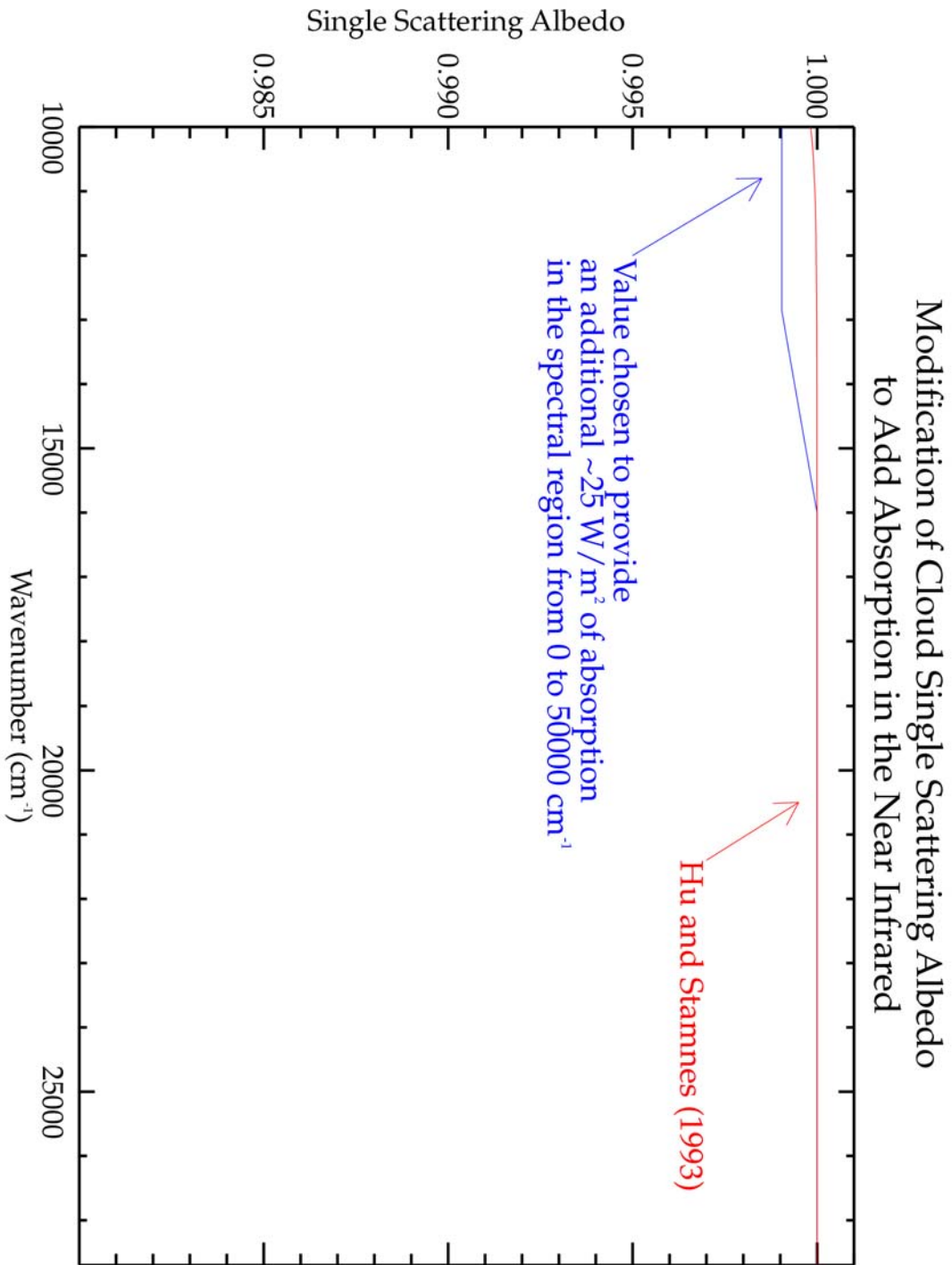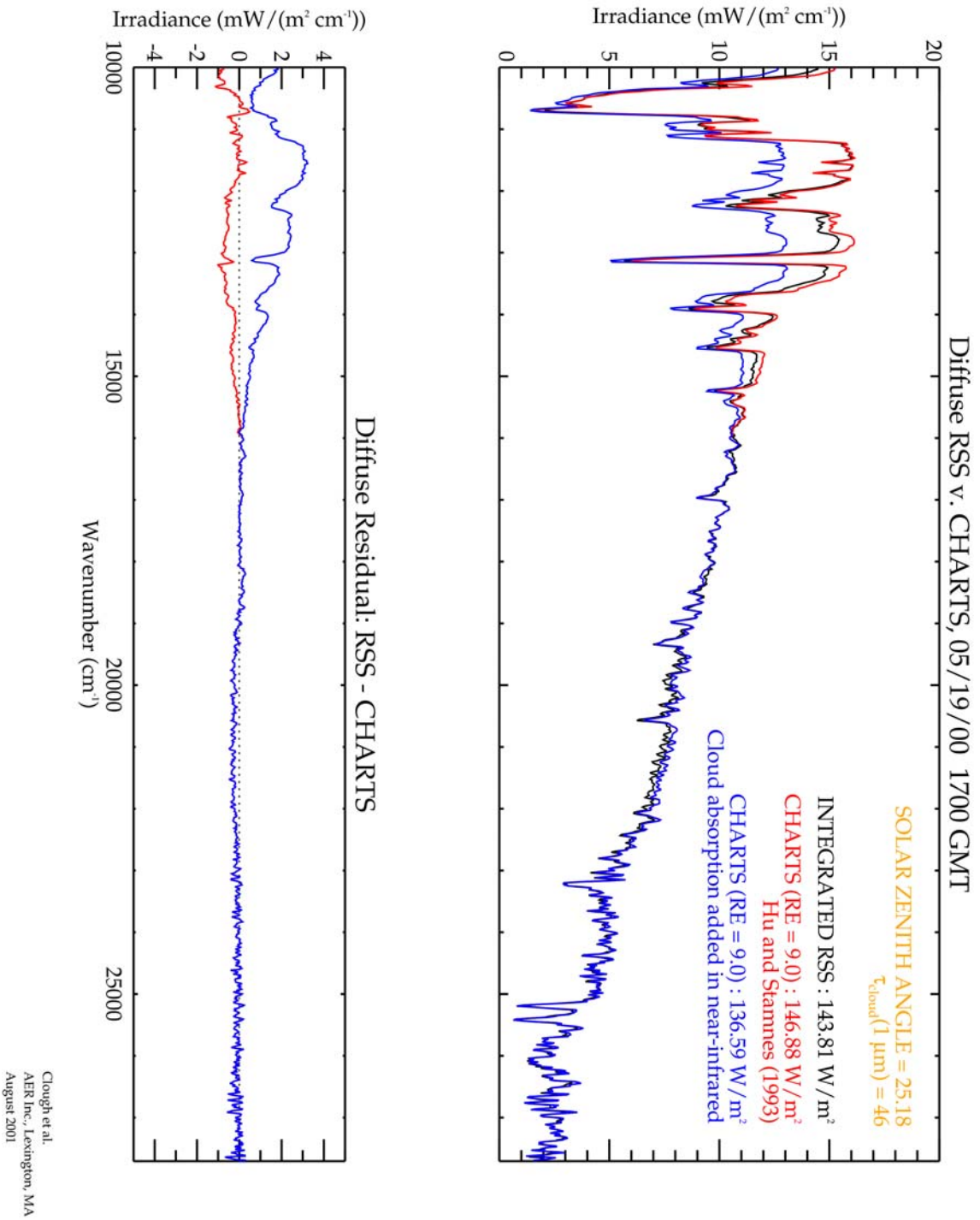
Figure 13.

Figure 14.

Mlawer, E. J., P. D. Brown, S. A. Clough, L. C. Harrison, J. J. Michalsky, P. W. Kiedron, and T. Shippert, 2000: Comparison of spectral direct and diffuse solar irradiance measurements and calculations for cloud-free conditions. *Geophys. Res. Lett.*, **27**, 2653-2656.

Moncet, J. -L. and S. A. Clough, 1997: Accelerated monochromatic radiative transfer for scattering atmospheres: Application of a new model to spectral radiance observations. *J. Geophys. Res.,* **102**, 21,853-21,866.